Earth and Planetary Science Letters, 114 (1993) 463–475
Elsevier Science Publishers B.V., Amsterdam

[CH]

Carbonatite metasomatism in the northern Tanzanian mantle: petrographic and geochemical characteristics

Roberta L. Rudnick [a], William F. McDonough [a] and Bruce W. Chappell [b]

[a] *Research School of Earth Sciences, The Australian National University, GPO Box 4, Canberra, A.C.T. 2601, Australia*
[b] *Department of Geology, The Australian National University, GPO Box 4, Canberra, A.C.T. 2601, Australia*

Received September 4, 1992; revision accepted December 15, 1992

ABSTRACT

Peridotite xenoliths from the Olmani cinder cone, northern Tanzania, possess distinctive mineralogical and chemical features interpreted to result from interaction of ultra-refractory peridotite residues with carbonatite melts. Chief among these are as follows: (1) The presence of unusually low Al_2O_3 clinopyroxene and the lack enstatite in refractory dunites (with olivines up to Fo_{94}). (2) The presence of monazite and F-rich apatite in refractory harzburgite and wehrlite xenoliths, respectively. (3) LREE enrichment and strong Ti depletion relative to Eu in all but one peridotite. Ca/Al ratios of the clinopyroxene-bearing dunites are some of the highest ever measured for peridotites (up to 10.8, relative to chondritic Ca/Al of 1.1). In addition, Zr/Hf and Ca/Sc ratios correlate positively, increasing with greater influence of carbonatite on the whole rock. (4) Clinopyroxene-bearing samples have a restricted range of isotopic compositions ($\epsilon_{Nd} = +3.1$ to $+3.9$, $^{87}Sr/^{86}Sr = 0.7034$ to 0.7035), whereas the monazite-bearing harzburgite has lower ϵ_{Nd} (+0.8) at similar $^{87}Sr/^{86}Sr$. The isotopic compositions of the former are similar to young, isotopically primitive east African carbonatites and basalts, suggesting the metasomatism occurred recently and that the carbonatites responsible for the metasomatism were ultimately derived from the asthenosphere.

Inferred trace element signatures of carbonatite melts responsible for modal metasomatism of these and other peridotites include: high La/Yb, Nb/La and Ca/Al, very high Zr/Hf and very low Ti/Eu; features similar to those of erupted carbonatites and consistent with partition coefficients for silicates in equilibrium with carbonatite melts. These trace element systematics are used to illustrate that many LREE-enriched spinel peridotite xenoliths may have been affected by addition of very small amounts ($\leq 2\%$) of carbonatite. Such metasomatism will have small effects on major element compositions of peridotites (e.g., Mg#, Ca/Al) relative to their trace element compositions. Whereas most LREE-enriched peridotites from the literature can be modeled as mixtures between carbonatite and refractory peridotite, the modally metasomatized Olmani peridotites and SE Australian wehrlites require an open-system style of metasomatism, perhaps due to higher proportions of carbonatite melt.

1. Introduction

Carbonatite melts have very low viscosities [1] and may be effective agents for transporting incompatible trace elements in the upper mantle [2,3]. Until recently [4,5], however, their interaction products with peridotites have remained largely undocumented. It is thus uncertain (1) what the trace element signatures of mantle-derived carbonatites are and (2) how important carbonatites are in controlling the incompatible trace element budget in the lithospheric mantle.

Here we describe refractory peridotite xenoliths from the Olmani cinder cone, northern Tanzania, that appear to be products of multiple interaction of asthenospheric-derived carbonatite melts with ultra-refractory lithospheric residues. This interaction has resulted in distinctive mineralogical and trace element signatures as well as uniform isotopic compositions in the peridotites. The chemical data are used to infer the trace element signatures of mantle-derived carbonatites and to evaluate the overall importance of carbonatite metasomatism in the lithospheric mantle.

2. Geology and samples

The Olmani cinder cone is part of the Neogene volcanism associated with the southern end

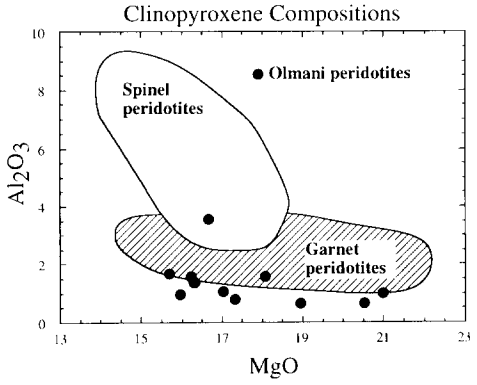

Fig. 1. MgO versus Al_2O_3 for Olmani clinopyroxenes compared with those from spinel and garnet peridotites. Olmani data from [8], data for fields from literature.

of the Gregory Rift Valley. These volcanics are comprised of basalt–phonolite–nephelinite lavas and, at some of the younger centers, carbonatite [6]. The Olmani cone is an ankaramite, similar in composition to the nearby Lashaine cinder cone and carries a variety of spinel-bearing peridotites [7,8].

Separate suites of Olmani peridotites have been described by Jones et al. [7] and Rudnick et al. [8]. The latter, which form the basis of the current study, consist of dunites (5 in total), one wehrlite and one harzburgite. In comparison, the suite of Jones et al. consists mainly of harzburgites (7) and dunites (6); they also describe two lherzolites and a single wehrlite. The Olmani peridotites are fresh and have coarse-equant to mosaic porphyroclastic textures. A striking feature of all of the dunites is the presence of clinopyroxene and absence of enstatite. Most Olmani peridotites are extremely refractory, containing chromites (Cr# = 100R/(Cr + Al) = 80 to 90) and highly magnesian olivines (Fo = 100g/(Mg + Fe) = 93 to 94) [7,8]. Exceptions are two Fe-rich clinopyroxene-bearing dunites from our collection that have Fo = 88 and 91, one of which, 89-778, is also unique in its trace element composition, described below. Clinopyroxenes are chrome diopsides with low Al contents compared with those from other spinel or garnet peridotite xenoliths (Fig. 1) [8]. The Olmani peridotites are generally free of hydrous phases, but contain variable amounts of alkali- and phosphorus-rich glass that may have formed by partial melting of apatite and hydrous phases in the presence of CO_2-rich fluids [7]. In several dunites clinopyroxene is concentrated within patches or along veins, and it commonly rims chromite. In the wehrlite, fluorine-rich apatite occurs as elongate, euhedral crystals that cross-cut vugs that also contain minute euhedral olivines, larger clinopyroxenes and a milky yellow, vesicular material (glass) that exhibits desiccation-like cracks (Fig. 2A and [8]). The single harzburgite from our suite is free of clinopyroxene and contains monazite. The monazite (10 wt.% ThO, 25% LaO) occurs as oval inclusions within olivine (Fo_{94}) near a grain boundary with enstatite (Fig. 2B). This is the first reported occurrence of monazite in a peridotite.

3. Analytical techniques

Major and trace element analyses are given in Table 1. Major and some trace element concentrations (V, Ni, Cu, Zn, Ga, Rb, Sr, Y, Zr) were determined by XRF [9,10]. Na_2O, Sc, Co, Cr and Ba were determined by INAA [11]. The remain-

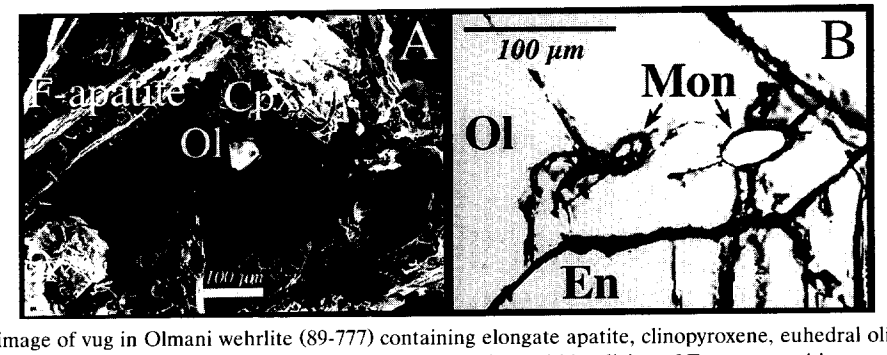

Fig. 2. (A) SEM image of vug in Olmani wehrlite (89-777) containing elongate apatite, clinopyroxene, euhedral olivine and cracked glass coating. (B) Plane polarized photomicrograph of monazite inclusions within olivine of Fo_{94} composition, near grain boundary with enstatite in Olmani harzburgite (89-773).

TABLE 1

Major (wt.%) and trace element (ppm) concentrations of Olmani peridotite xenoliths

Sample	89-772	89-773	89-774	89-776	89-777	89-778	89-780
Rock type	dunite	harz	dunite	dunite	wehrlite	dunite	dunite
Modal Ol	96.5	82.0	99.1	96.4	91.9	98.2	97.6
Mg # Ol	88	94	93	94	90-94	91	94
SiO_2	40.60	44.01	41.30	41.79	41.35	41.03	41.47
TiO_2	0.02	0.01	0.00	0.02	0.05	0.05	0.03
Al_2O_3	0.11	0.39	0.10	0.09	0.17	0.22	0.12
FeOt	12.47	5.97	6.26	5.87	8.52	8.85	6.72
MnO	0.15	0.08	0.08	0.09	0.16	0.11	0.10
MgO	46.06	49.12	51.88	51.65	48.20	49.69	50.98
CaO	0.66	0.11	0.16	0.58	1.36	0.28	0.48
Na_2O *	0.053	0.025	0.032	0.054	0.069	0.016	0.034
K_2O	–	0.03	0.02	–	–	0.01	0.01
P_2O_5	–	0.01	0.05	0.01	0.18	–	0.01
S	–	0.01	0.01	0.01	0.02	–	0.02
Total	100.24	99.88	100.01	100.3	100.22	100.34	100.12
Mg #	86.8	93.6	93.7	94.0	91.0	90.9	93.1
Ca/Al	8.10	0.38	2.16	8.69	10.8	1.71	5.40
Sc *	4.9	4.1	1.6	1.7	2.9	3.3	2.1
V	11	16	7	7	14	6	8
Cr *	940	2500	1890	1920	2420	640	2020
Co *	180	112	128	120	121	200	123
Ni	3770	2480	2810	2890	2540	3930	2790
Cu	19	2	–	2	–	10	4
Zn	89	39	40	44	90	64	55
Ga	0.4	0.3	0.2	0.2	0.6	0.5	0.6
Rb SSMS	0.3	5.0	0.9	0.2	0.4	1.3	1.2
Rb XRF	0.1	3.9	0.7	0.1	0.1	0.7	1.4
Sr SSMS	10.8	17	6.8	9.9	32.7	43.8	12.8
Sr XRF	7.7	15.6	5.1	8.3	29.5	32.5	12.6
Y SSMS	0.50	0.39	0.30	0.68	3.10	0.47	0.81
Y XRF	0.4	0.4	0.2	0.7	2.3	0.5	0.7
Zr SSMS	1.3	1.0	0.9	7.9	13.4	4.1	6.1
Zr XRF	1.2	0.7	0.8	7.4	10.5	3.0	6.6
Nb	0.7	1.5	1.2	1.1	1.8	2.5	1.2
Ba	4.0	110	7.0	3.2	6.2	29.0	17.3
Ba *	10	116	10	–	10	30	20
Cs	0.005	0.009	0.012	0.007	0.007	0.015	0.008
La	0.36	7.39	0.13	0.40	3.45	1.09	0.43
Ce	1.39	9.70	0.47	1.35	10.1	1.90	1.72
Pr	0.17	0.73	0.056	0.20	1.51	0.19	0.25
Nd	0.68	2.01	0.20	0.89	6.91	0.64	1.12
Sm	0.13	0.19	0.041	0.21	1.31	0.099	0.27
Eu	0.036	0.043	0.012	0.063	0.35	0.023	0.079
Gd	0.09	0.11	0.038	0.16	0.87	0.061	0.21
Tb	0.015	0.006	0.024	0.105	0.008		
Dy	0.092	0.153	0.191				
Ho	0.018	0.017	0.008	0.030	0.085	0.013	0.034
Er	0.040	0.04	–	0.058	0.132	0.036	0.078
Yb	0.034	0.04 *	–	0.043	0.065	–	0.048
Hf	0.029	0.040	0.021	0.076	0.135	0.078	0.091
W	0.07	0.08	0.05	0.08	0.05	0.06	0.07
Th	0.03	1.56	–	0.022	0.056	0.108	0.021
U	–	0.055	0.105	0.010	0.046	0.022	–
Zr/Hf	44.8	25.0	42.9	103.9	99.3	52.6	67.0

* Data from INAA, – = below detection limits, SSMS = spark source mass spectrometry, XRF = X-ray fluorescence.

ing trace elements (plus additional analyses of Rb, Sr, Y, Zr and Ba) were analyzed by MS7 spark-source mass spectrometry [8]. Improved resolution in the MS7 has allowed the deconvolution of Mg- and/or C-based molecular interferences from certain isotopes (i.e., ^{89}Y, ^{93}Nb, ^{133}Cs). These interferences are only significant in samples with low concentrations of these elements, such as the peridotites reported here. Accuracy, as determined by replicate analyses of international standards, is better than 10%; precision is generally better than 5%.

Sr and Nd isotopic analyses for clinopyroxene separates and whole rocks are given in Table 2. Clinopyroxenes were hand picked to optical purity then acid leached. Procedures for leaching and isotopic measurements are given in [12].

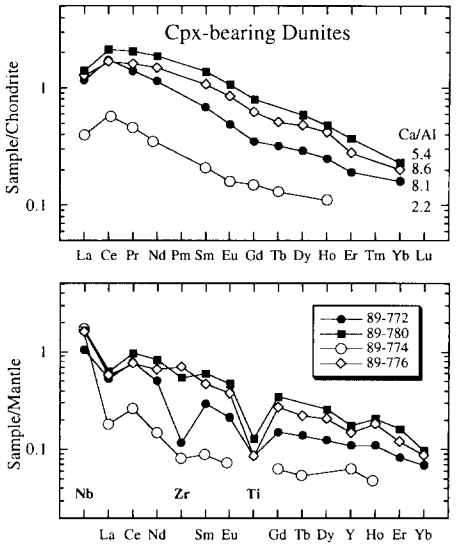

Fig. 3. REE and mantle-normalized trace element patterns for Olmani clinopyroxene-bearing dunites. Ordinary chondrite values from [41], and mantle normalizing values from [17].

4. Chemical and isotopic compositions

Major and trace element compositions of the Olmani peridotites reflect refractory residues enriched in CaO and incompatible trace elements (Table 1). MgO and Ni concentrations are high and SiO_2, Al_2O_3, FeO and TiO_2 contents are low compared with other spinel peridotite xenoliths from alkali basalts [9]. For all but the harzburgite, CaO concentrations are markedly higher than other peridotites of similar MgO contents, reflecting the abundance of clinopyroxene in these otherwise depleted samples. Ca/Al ratios are thus high (1.75 to 10.8) relative to the primitive mantle value of 1.1 [13] or the median spinel peridotite value of 1.35 [14]. The harzburgite also has high MgO and Ni contents, but low CaO and Ca/Al, reflecting its ultra-depleted character and lack of clinopyroxene.

All samples are enriched in LREE with the nature and degree of enrichment reflecting the modal mineralogy. Clinopyroxene-bearing dunites, except for 89-778, exhibit a distinctive concave downward pattern in the lightest REE (i.e., $La_n < Ce_n$) (Fig. 3). The overall abundance of the REE in these dunites correlate roughly with their Ca/Al ratios (hence clinopyroxene content); samples with lowest Ca/Al have the lowest REE abundances. The apatite-bearing wehrlite (89-777) has high REE concentrations and, compared with the dunites, has a less con-

TABLE 2

Sr and Nd isotopic compositions of Olmani peridotites

		Rb (ppm)	Sr (ppm)	$^{87}Rb/^{86}Sr$	$^{87}Sr/^{86}Sr$	2σ	Nd (ppm)	Sm (ppm)	$^{147}Sm/^{144}Nd$	$^{143}Nd/^{144}Nd$	2σ	ϵ_{Nd}
89-772	cpx	0.096	145.7	0.0019	0.70340	2				0.512822	20	3.6
89-773	wr		15.0		0.703811	15	2.035	0.207	0.0615	0.512680	16	0.8
89-774	cpx	0.554	127.5	0.0126	0.70347	1	13.97			0.512805	20	3.3
89-777	wr		28.2		0.703502	18	6.412			0.512840	12	3.9
	cpx	0.068	360.5	0.0005	0.703468	17	59.01	15.55	0.1593	0.512798	10	3.1
89-778	cpx		70.9		0.703875	16	5.039			0.512811	14	3.4

cpx = clinopyroxene separate, wr = whole rock. Value for repeat analyses of NBS987 is 0.710229 ± 16, for n-Nd-1 is 0.512178 ± 8 and for BCR-1 is 0.512649 ± 10. Errors reported as 2σ.

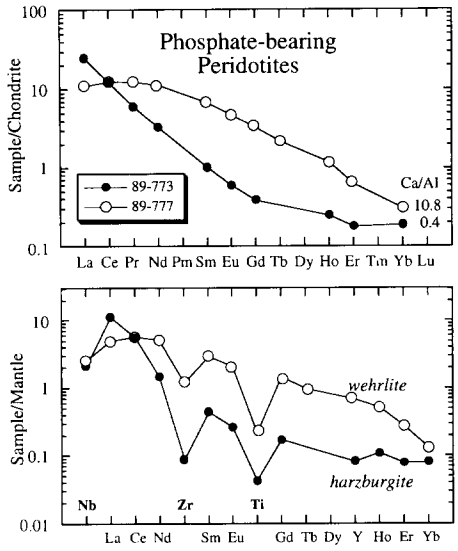

Fig. 4. REE and mantle-normalized trace element patterns for Olmani phosphate-bearing peridotites.

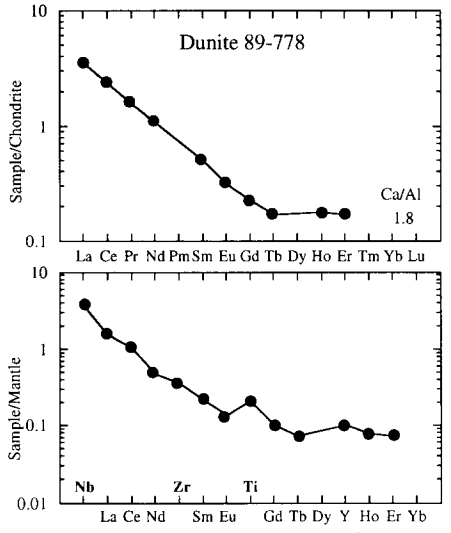

Fig. 5. REE and mantle-normalized trace element patterns for Olmani clinopyroxene-bearing dunite 89-778.

cave LREE pattern (Fig. 4). We believe this reflects the influence of apatite, in addition to clinopyroxene, on the bulk rock composition. The monazite-bearing harzburgite (89-773) shows extreme fractionation of light to heavy REE ($(La/Yb)_N = 130$) and strong enrichment of the REE (Fig. 4) and Th relative to other incompatible trace elements. These features reflect the influence of monazite on the whole rock composition.

On mantle-normalized diagrams, high field strength elements (HFSE) show variable depletions or enrichments relative to the REE (Figs. 3 and 4) (with 89-778 again an exception, Fig. 5). Ti is depleted relative to Eu in all samples, whereas Zr and Hf may or may not be depleted compared with Sm. Nb is enriched compared to La in all dunites, but is depleted relative to La in the phosphate-bearing peridotites. Zr/Hf ratios vary from near chondritic (38) to very high values (up to 100), correlating with both Zr abundance and Ca/Sc ratio (Fig. 6).

Ratios of Zr/Hf, Y/Ho and Nb/Ta are believed to be chondritic in basalts, komatiites and peridotites from the Earth [15,16,17]. This is because both elements (numerator and denominator) show similar geochemical behavior as a result of their nearly identical ionic radii and charge. Thus, most geochemists are cautious about accepting reports of marked fractionation in these element pairs. (There is evidence for Zr/Hf and Nb/Ta fractionation in lunar rocks, although the

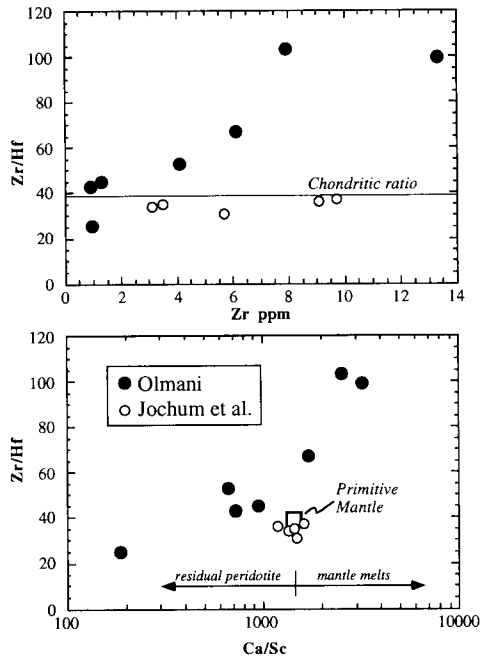

Fig. 6. Zr versus Zr/Hf and Ca/Sc vs. Zr/Hf for Olmani peridotites. Data for other well-measured spinel peridotites from [16]. Range of Ca/Sc for mantle melts (with Ca/Sc increasing in the direction MORB < alkali olivine basalts < nephelinites < kimberlites ≈ carbonatites) and residual peridotites shown for reference.

cause of this variation remains unclear; see Jochum et al [15].) The Olmani peridotites exhibit a wide range of Zr/Hf ratios, which is beyond analytical uncertainties. In contrast, Y/Ho ratios in the Olmani samples do not differ significantly from the chondritic value (Table 1), as is true for a large number of peridotites [14,16]. As of yet, we have no data of Nb/Ta ratio in the Olmani peridotites. Large variations in Zr/Hf and Nb/Ta ratios in peridotites from the literature [14], may in part reflect errors in the analyses at these low concentrations. However it is possible that some of this variation is due to mantle processes. Recently, Dupuy et al. [18] have highlighted fractionated Zr/Hf ratios in intraplate basalts and carbonatites.

There is marked homogeneity in the Sr and Nd isotopic compositions of the clinopyroxene-bearing Olmani peridotites, falling within the range $^{87}Sr/^{86}Sr = 0.70340$ to 0.70350 (excluding 89-778) and $\epsilon_{Nd} = +3.1$ to $+3.9$ (Table 2). Such homogeneity contrasts with the large $^{87}Sr/^{86}Sr$ and ϵ_{Nd} ranges often found in peridotite xenoliths from a single vent [e.g. 12,19]. The monazite-bearing harzburgite has similar $^{87}Sr/^{86}Sr$ but significantly lower ϵ_{Nd} compared to the clinopyroxene-bearing Olmani peridotites. Recent basalts and carbonatites from east Africa define two subparallel fields on the Sr versus Nd isotope plot (Fig. 7) (the significance of the separation between these two rock types is, as of yet, not understood). The clinopyroxene-bearing peridotites fall near the boundary of these fields at $\epsilon_{Nd} = +3$, whereas the monazite-bearing harzburgite falls at lower ϵ_{Nd} values, well within the carbonatite field.

Clinopyroxene-bearing dunite 89-778 exhibits several unique chemical features: it has a lower Mg# than the majority of the dunites, it does not show the concave-downwards pattern in the LREE (typical of the other dunites), HFSE are not fractionated relative to the REE in this sample and it has a slightly higher $^{87}Sr/^{86}Sr$ compared with the other samples (Figs. 5 and 7). In addition, the clinopyroxenes in this sample have considerably higher Ti and Al and lower Na_2O than those in the other dunites [8]. The mineralogy of 89-778 and its high Zr/Hf and Ca/Sc ratios are the only features it shares with the other dunites. Because of the inherent differences of this sample, it will not be included in the following discussion on the origin of the clinopyroxene-bearing peridotites. This sample may have originated as the others, but subsequently interacted with a silicate melt.

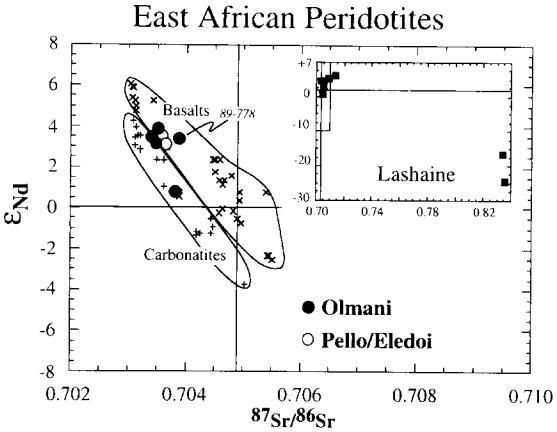

Fig. 7. Initial $^{87}Sr/^{86}Sr$ versus ϵ_{Nd} of Olmani peridotites ($T = 0$) compared with fields of Cretaceous–Tertiary east African carbonatites [28,42] and Quaternary–Tertiary alkali basalts [43–47]. Inset shows isotopic data for mineral separates from Lashaine peridotites ([19] and McDonough, unpublished data).

5. Discussion

We envisage the Olmani peridotites to be the products of interaction of carbonatite melts with ultra-refractory residues. The latter may have been formed by extraction of large degree partial melts (e.g., komatiites) or by several stages of melting of a primitive mantle composition, leaving behind clinopyroxene-free harzburgites and dunites with high Mg numbers [8]. The timing of this depletion is unknown. These residues were subsequently modified by exchange and interaction with carbonatite melts, to produce their distinctive mineralogy and chemistry.

5.1 The case for carbonatite metasomatism

The similarity in Sr and Nd isotopic compositions of the clinopyroxene-bearing Olmani peridotites suggests that they recently equilibrated with a single magma or several closely related magmas. The presence of clinopyroxene and absence of enstatite in otherwise refractory dunites suggest that the clinopyroxene is a secondary

mineral formed at the expense of primary enstatite [4]. The low Al and high Mg# of these clinopyroxenes relative to those in other metasomatized peridotites suggests that the melt responsible for their crystallization carried little Fe or Al. Silicate melt metasomatism associated with pyroxenite veins is characterized by Fe-enrichment and a general addition of Al, Ca, and Ti [20,21]. In the Olmani clinopyroxene-bearing peridotites the only major element added in significant quantities as a result of the metasomatism is Ca. This melt also carried significant phosphorus and REE, as evidenced by the intergrowth of apatite and clinopyroxene. The above features are consistent with carbonatite melt metasomatism [2].

Apatite mineral chemistry is also consistent with carbonatite metasomatism having occurred in these peridotites. Recent partitioning data for apatite in equilibrium with carbonate melt show that F is partitioned into apatite ($K_D \sim 1.1$) whereas Cl is not ($K_D \sim 0.1$) [22]. If erupted carbonatites are used as analogs to primary carbonatite melts from the mantle, then their F/Cl ratios of ~ 1.0 to $\gg 1$ [23] indicate that apatites precipitated from carbonatite melts will be F-rich and Cl-poor. This is true for apatites in erupted carbonatites [24] and also in the Olmani peridotites [8].

Monazite in the Olmani harzburgite is also best explained as being produced by carbonatite metasomatism. However in this case the lack of Ca in the resultant metasomatized peridotite (i.e. absence of clinopyroxene and formation of monazite rather than apatite) suggests that the carbonatite was magnesitic. The reaction enstatite + magnesite = magnesian olivine + CO_2 [25] and the presence of monazite in Fo_{94} olivine near a grain boundary with enstatite (Fig. 2) are consistent with monazite precipitation from a magnesite carbonatite melt as the melt reacted with the enstatite to form olivine. This, coupled with the distinctive isotopic composition of this sample relative to the other Olmani peridotites, suggests that at least two episodes of carbonatite metasomatism occurred beneath Olmani.

5.2 Chemical characteristics of the carbonatite

The REE compositions of these peridotites do not directly reflect the composition of the metasomatizing melt if metasomatism occurred in an open system. The distinctive concave-downward LREE pattern of the clinopyroxene-bearing dunites suggests that it was open-system. However, the carbonatite melt composition can be calculated using relevant partition coefficients [26,27] and the peridotites' modal mineralogies [8]. Since there are no partition coefficients available for apatite or monazite in equilibrium with carbonatitic melts, our discussion is limited to the phosphate-free peridotites. In these samples, clinopyroxene will be the main host of the REE and the bulk partition coefficient can be calculated from the modal abundances. Our calculations indicate that the coexisting melt was LREE-enriched with Ce equal to 250–600 times chondrite and Yb equal to 8–15 times chondrite, similar to a number of erupted east African carbonatites [28]. In contrast, Ba and Cs concentrations in the coexisting melt calculated in a similar fashion are much higher than those found in carbonatite melts (13,000–83,000 ppm Ba and 90–150 ppm Cs compared with < 3500 ppm Ba and < 7 ppm Cs in carbonatites [28]). This may indicate that significant alkali elements are concentrated on grain boundaries [e.g., 29].

The distinctive HFSE fractionations relative to the REE in the Olmani peridotites may reflect the chemical characteristics of the carbonatites and/or the partitioning behavior of HFSE between carbonatite melt and the reaction products of carbonatite metasomatism (clinopyroxene and phosphates). HFSE depletions in both phosphate-bearing samples reflect the preferential partitioning of REE over HFSE into the phosphates. In the phosphate-free samples the HFSE patterns probably reflect both clinopyroxene-melt partitioning and the characteristics of the metasomatizing melt. Partition coefficients for Ti in clinopyroxene in equilibrium with basaltic melts are slightly lower than for Eu [30]. In contrast, Ti partition coefficients for clinopyroxene in equilibrium with carbonatitic magmas show the opposite behavior relative to Eu, i.e., Ti enters the clinopyroxene in preference to Eu [31]. Thus, if the liquid from which the Olmani clinopyroxenes precipitated was carbonatite, it had and even greater Ti depletion relative to Eu than currently exhibited by the Olmani peridotites.

Strong Zr, Hf and Ti depletions and Nb en-

richments relative to the REE, and high Zr/Hf ratios, are characteristic of many erupted carbonatites [18,28]. In addition, experimental partitioning studies demonstrate that primary carbonatites will be depleted in Ti relative to the middle REE [31,32]. It is therefore likely that these HFSE fractionation patterns in the peridotites reflect the characteristics of the metasomatizing carbonatite melt. The progressive increase of Zr/Hf with Ca/Sc in the Olmani peridotites (Fig. 6) reflects increasing influence of the carbonatite melt on the whole rock chemistry. This melt was strongly LREE-enriched, had low Ti/Eu, high Nb/La, Ca/Sc and very high Zr/Hf.

The HFSE/REE fractionations observed in carbonatites are generally attributed to late-stage crystal fractionation [28]. Their presence in the Olmani peridotites suggests that if they are indeed due to crystal fractionation, then this fractionation occurred within the mantle beneath northern Tanzania (requiring the precipitation of a HFSE-bearing, REE-poor phase). Alternatively, recent partitioning data for silicate minerals in equilibrium with carbonatite melt indicate that the HFSE/REE fractionations observed here (i.e., Ti depletion relative to Eu and Zr depletion relative to Sm) may be produced by residual garnet, clinopyroxene and/or amphibole in the source of carbonatite magmas [27,31,32]. In addition, higher partition coefficients for Ta compared with Nb for silicates in equilibrium with carbonatite melt increase the Nb/Ta ratios in the carbonatite relative to chondrite or primitive mantle [27,32]. A similar effect may explain the fractionation of Zr from Hf observed here.

5.3 Timing of metasomatism and source of the carbonatite

As demonstrated above, the REE budget of the Olmani peridotites is dominated by the carbonatite component. Thus their present Nd isotopic compositions reflect that of the carbonatite melt and the time since metasomatism. The Olmani peridotites are all strongly LREE-enriched, some extremely so. Their Nd isotopic compositions will therefore be retarded relative to a chondritic mantle with time. The similarity of Nd isotopic compositions between the clinopyroxene-bearing peridotites and some of the more isotopically primitive east African carbonatites and basalts (Fig. 7) suggests that the metasomatism in these samples was associated with this Tertiary to Recent volcanism. The unequilibrated textures of many of the peridotites (e.g., clinopyroxene- and apatite-filled veins, Fig. 2) lend support to this. In contrast, the lower ϵ_{Nd} of the monazite-bearing harzburgite may indicate recent metasomatism by a carbonatite derived from a different source, similar to that for some of the more isotopically evolved east African carbonatites (Fig. 7).

These isotopic compositions may be used to make inferences on the source of the carbonatite. If the carbonatite melts were generated in the lithospheric mantle, their Nd isotopic compositions (and the composition of the metasomatized peridotites) should represent the average isotopic composition of that mantle source. LREE enrichment is ubiquitous in the east African lithospheric mantle; peridotites from the nearby Lashaine cinder cone are all LREE-enriched ([33]; Rudnick et al., unpubl. data) and have variably evolved Nd and Sr isotopic compositions of $\epsilon_{Nd} = +3$ to -22 and $^{87}Sr/^{86}Sr = 0.7047$ to 0.8360 ([19]; McDonough, unpubl. data). None of these samples plot in the upper left quadrant of the $^{87}Sr/^{86}Sr$ vs. ϵ_{Nd} diagram (Fig. 7). The uniform isotopic compositions of the Olmani clinopyroxene-bearing peridotites at $\epsilon_{Nd} = +3$ and $^{87}Sr/^{86}Sr = 0.7035$, coupled with the absence of samples from the east African mantle with Nd values greater than $+3$, is evidence in support of an asthenospheric origin for the carbonatite responsible for the metasomatism. Two alternatives are therefore viable: (1) the carbonatite was generated by melting lithosphere that had become recently carbonated (and completely overprinted in incompatible elements) by asthenosphere-derived intraplate melts [e.g., 5, 34] or (2) the carbonatites themselves originated in the asthenosphere either as discrete melts or possibly exsolved from silica undersaturated intraplate magmas [e.g., 35].

5.4 Comparison with other areas

Yaxley et al. [4] describe peridotite xenoliths from southeast Australia that they interpreted as having interacted with carbonatite melts. There are both similarities and differences between the

Olmani and Australian examples. In addition to clinopyroxene and apatite, pargasitic amphibole is associated with the metasomatism in the Australian case, and clinopyroxenes are rich in Na compared with the Olmani examples. These features suggest that the carbonatite responsible for metasomatism in the SE Australian mantle was hydrous and considerably more sodic than in the Olmani example. This illustrates that there are probably a spectrum of carbonatite melt compositions, which vary with pressure and temperature of melting and the composition of the source from which they were derived. In addition, the peridotite protoliths in Australia are not as depleted as are the Olmani peridotites, leading to higher Mg numbers and more extreme Ca/Al ratios in the latter. Features common to both peridotite suites include elevated Ca/Al ratios relative to both primitive mantle or average spinel peridotites and extreme enrichments in REE and Nb, and relative depletion in Ti, Zr and Hf. Both suites also exhibit isotopic compositions similar to young volcanic activity in their respective areas.

In addition to the above study, peridotite xenoliths from Algeria and the Eifel, Germany, are interpreted to have experienced carbonatite metasomatism. Dautria et al. [5] describe dunites and harzburgites that contain Cr diopside-rich aggregates surrounding spinels that they interpret to have crystallized by reaction of carbonatitic liquids with harzburgites and dunites. Thibault et al. [34] suggested a similar interpretation for xenoliths from Gees crater, the Eifel, on the basis of increasing clinopyroxene contents in lherzolites and wehrlites at uniformly high Mg#.

5.5 *The importance of carbonatite metasomatism*

The recognition of carbonatite metasomatism in four regions of the lithospheric mantle with widely differing geologic histories leads to the question of how widespread such metasomatism may be. Baker and Wyllie [3] have recently suggested that carbonatite metasomatism may be responsible for the commonly observed LREE enrichment of refractory peridotites (i.e., carbonate melt may be component 'B' of Frey and Green [36]). They showed that addition of very small amounts of carbonatite melt will have a dramatic effect on both P_2O_5/TiO_2 and LREE enrichment in peridotitic residues.

This study and that of Yaxley et al. [35] have documented geochemical features characteristic of mantle-derived carbonatite melts. These include high La/Yb, very high Zr/Hf, very low Ti/Eu and, of course, high Ca/Al. Although none of these features are individually unique to carbonatites (save, perhaps high Zr/Hf, for which very few quality peridotite data are available in the literature), taken in concert, they provide a set of criteria which can be used to test the importance of carbonatite metasomatism in the upper mantle.

The geochemical signature imparted to a peridotite by a carbonatite melt will depend upon whether the metasomatism is accomplished by closed-system addition of carbonatite into peridotite, or by open-system reaction between carbonatite melt and peridotite. The former would impart carbonatite composition in relation to the proportion of melt added, and is easily modeled by bulk mixing. In contrast, the latter is more difficult to quantify as it depends upon the amount and nature of the phases formed during the metasomatism and the partition coefficients for trace elements between these phases and carbonatite melt. Bulk mixing has been advocated as likely on the basis of decarbonation reactions that occur when carbonatite melt enters a peridotite [3]; however, it is not clear that bulk mixing would still occur if the melt to rock ratio is high. To facilitate modeling, bulk mixing is assumed in the following discussion unless otherwise stated.

Figure 8 plots the degree of Ti depletion against the degree of LREE enrichment in spinel peridotite xenoliths from the literature; peridotites interpreted as having experienced carbonatite metasomatism are delineated separately. The Olmani peridotites and SE Australian wehrlites show the highest $(La/Yb)_N$ and lowest Ti/Eu of the data set. In addition, many SE Australian peridotites from the literature show similarly high $(La/Yb)_N$ and low Ti/Eu. The entire data set exhibits a rough negative trend. This trend has been suggested by Kelemen et al. [30] to be due to reaction of primitive basaltic melt with lherzolite to form harzburgite. They attributed the low Ti/Eu (or Ti/Ti* in their paper) to crystallization of enstatite from a melt

already Ti-depleted due to previous precipitation of enstatite.

We suggest an alternative interpretation: that the trend may be produced by mixing small amounts of carbonatite melt into refractory harzburgite. One possible model is illustrated in Fig. 8B. Harzburgite formed by extraction of large degrees of partial melt from a relatively primitive peridotite will have super-chondritic Ti/Eu, because enstatite in equilibrium with basalt has a higher K_d for Ti than for Eu [37]. For example, harzburgite D-50 of Stosch [38] has Ti/Eu = 20,000 and a uniformly low and flat REE pattern. Mixing only 0.5% carbonatite (here assumed to be equal to the average Ca-carbonatite of Wooley and Kempe [39]) into such a harzburgite can explain the Ti–REE compositions of most spinel peridotite xenoliths from the literature. Only peridotites showing 'modal' carbonatite metasomatism from SE Australia and Olmani require

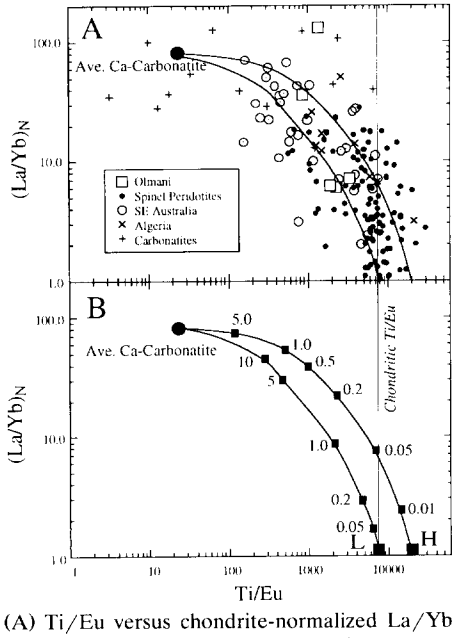

Fig. 8. (A) Ti/Eu versus chondrite-normalized La/Yb ratio for peridotite xenoliths from the literature (data set of [14]). Peridotites interpreted as having experienced carbonatite metasomatism are designated with different symbols, shown in key. Circles with dots in the middle are SE Australian wehrlites described by Yaxley et al. [4]. Also shown are individual carbonatite analyses [28] and average Ca-carbonatite [39]. (B) Same as in (A), but showing mixing curves between harzburgite (H) and pyrolitic lherzolite (L). Numbers adjacent to curves represent percentage of average carbonatite added to peridotites.

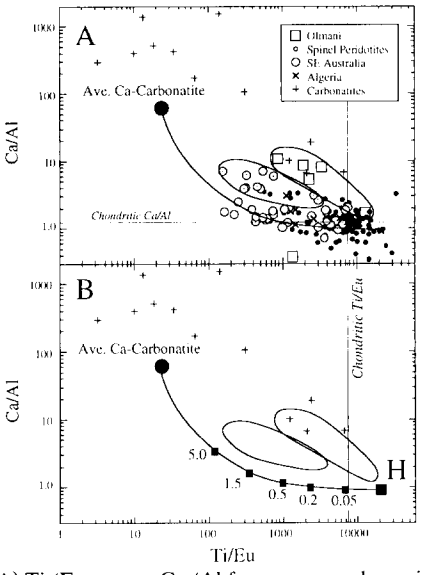

Fig. 9. (A) Ti/Eu versus. Ca/Al for same samples as in Fig. 8. (B) Mixing curves between harzburgite (H) and average carbonatite. Numbers adjacent to curves represent percentage of average carbonatite added to peridotites.

larger amounts of carbonatite (up to 5% addition, if formed by bulk mixing). Choosing a peridotite starting composition close to that of primitive mantle results in a mixing curve of the same general shape, but requires greater amounts of carbonatite to shift the trace element ratios to the same extent (Fig. 8B).

A possible test of this model is to determine whether peridotites with low Ti/Eu have higher modal clinopyroxene contents, which would be expected if these geochemical features are related to addition of Ca-carbonatite magma. Here we will use Ca/Al ratio as an indicator of the proportion of clinopyroxene to orthopyroxene in the whole rock. Figure 9 plots Ti/Eu against Ca/Al for the same peridotite data set; the Olmani peridotites and SE Australian wehrlites are shown as fields. There are two interesting observations about this diagram: (1) many of the SE Australia peridotites fall along a carbonatite–harzburgite mixing curve, with Ca/Al only moderately increased as Ti/Eu dramatically decreases, and (2) the fields for peridotites showing modal carbonatite metasomatism from Olmani and SE Australia are not intersected by the curve. The position of the curve does not change significantly if a carbonatite end-member with higher

Ca/Al is used (similar to many of the carbonatites reported in Nelson et al. [28]), or if a less refractory starting composition is used.

The failure of the bulk mixing line to pass through the field of the 'modally' carbonatite metasomatized peridotites from SE Australia and Olmani (Fig. 9) suggests that they did not form by simple mixing, but are more likely to represent reaction products of carbonatite melt with peridotite. Open system reaction between migrating carbonatite melt and peridotite matrix will result in the formation of clinopyroxene and olivine ($\pm$amphibole), at the expense of enstatite ($\pm$primary diopside and spinel) [4]. The Ca/Al of the reaction product will mainly reflect the clinopyroxene to orthopyroxene ratio of the metasomatized peridotite, whereas the Ti/Eu ratio will reflect the partitioning behavior of these elements between the newly created phases and the carbonatite melt. Partition coefficients for Ti are high relative to those for middle REE in clinopyroxene and amphibole in equilibrium with carbonatite [31,32]. If carbonatite metasomatism occurred in an open system, the Ti/Eu ratios of the peridotites thus formed would be higher than those in peridotites formed by simple bulk mixing at a given Ca/Al. This suggests that the amount of carbonatite melt responsible for the formation of the Australian wehrlites and Olmani dunites may be even greater than 5%. This, in turn, may suggest a link between the style of carbonatite metasomatism and the amount of melt available: at very low melt fractions, bulk mixing is the physical mechanism of carbonatite metasomatism but at higher melt volumes ($\geqslant 2\%$?) open-system reactions may predominate.

This analysis of the literature data suggests that the LREE enrichment seen in peridotite xenoliths is consistent with addition of small amounts of carbonatite melt to partial melting residues. Such metasomatism may be manifested in the formation of new mineral assemblages (hydrous, as in the SE Australian case or anhydrous as in the Tanzanian case) or, at very small melt fractions, may result in cryptic metasomatism. The latter will have enormous influence on the trace element compositions of peridotites, without significantly changing their major element characteristics (i.e., Mg# will remain high and Ca/Al ratios only increase slowly). Thus carbonatite metasomatism, which can be accomplished at exceedingly small melt fractions, should be considered in addition to silicate melt metasomatism in evaluating the origins of incompatible element enrichments in the lithospheric mantle. The distinctive trace element signature of carbonatites outlined here and in other studies [3,4,18,27,32,35] will facilitate in this evaluation.

5.6 Carbonatites in subduction settings?

One final hypothesis that may be tested by the trace element systematics discussed above is the suggestion that carbonatite metasomatism may be important in the sources of island arc basalts [32]. The carbonatites responsible for metasomatizing the Olmani and other peridotites were depleted in some HFSE relative to REE (i.e., Ti $\pm$ Zr and Hf), but were not depleted in Nb relative to La. Thus, metasomatism of a depleted mantle wedge by such a carbonatite would result in Nb enrichment, in contrast to the Nb depletion that is ubiquitous in island arc basalts [40]. It would also lead to elevated Zr/Hf (and Nb/Ta) in island arc basalts, in contrast to their observed chondritic ratios. We conclude that carbonatites of the type described above are unlikely to be important in the petrogenesis of convergent margin magmas.

Acknowledgements

We thank G. Yaxley, S.M. Eggins, P. Kelemen and A.E. Ringwood for discussions and suggestions. Review comments from H.-G. Stosch, P. Kelemen, F. Frey, G. Yaxley, R. Sweeney, F.R. Boyd and T.H. Green helped to improve the manuscript and are greatly appreciated.

References

1 E.B. Watson, J.M. Brenan and D.R. Baker, Distribution of fluids in the continental mantle, in: Continental Mantle, M.A. Menzies, eds., pp. 111–126, Oxford Univ. Press, Oxford, 1990.

2 D.H. Green and M.E. Wallace, Mantle metasomatism by ephemeral carbonatite melts, Nature 336, 459–462, 1988.

3 M.B. Baker and P.J. Wyllie, High-pressure apatite solubility in carbonate-rich liquids: implications for mantle metasomatism, Geochim. Cosmochim. Acta 56, 3409–3422, 1992.

4 G.M. Yaxley, A.J. Crawford and D.H. Green, Evidence for carbonatite metasomatism in spinel peridotite xenoliths from western Victoria, Australia, Earth Planet. Sci. Lett. 107, 305–317, 1991.
5 J.M. Dautria, C. Dupuy, D. Takherist and J. Dostal, Carbonate metasomatism in the lithospheric mantle: peridotitic xenoliths from a melilititic district of the Sahara basin, Contrib. Mineral. Petrol. 111, 37–52, 1992.
6 J.B. Dawson, Neogene tectonics and volcanicity in the North Tanzania sector of the Gregory Rift Valley: contrasts with the Kenya sector, Tectonophysics 204, 81–92, 1992.
7 A.P. Jones, J.V. Smith and J.B. Dawson, Glasses in mantle xenoliths from Olmani, Tanzania, J. Geol. 91, 167–178, 1983.
8 R.L. Rudnick, W.F. McDonough and A. Orpin, Northern Tanzanian peridotite xenoliths: a comparison with Kaapvaal peridotites and inferences on metasomatic interactions, in: Kimberlites, Related Rocks and Mantle Xenoliths, Vol. I (Proceedings of the 5th International Kimberlite Conference), H.O.A. Meyer and O. Leonardos, eds., pp. 336–353, 1992.
9 K. Norrish and B.W. Chappell, X-ray fluorescence spectrometry, in: Physical Methods in Determinative Mineralogy, J. Zussman, ed., pp. 201–272, Academic Press, London, 1977.
10 B.W. Chappell, Trace element analysis of rocks by X-ray spectrometry, Advances in X-Ray Analysis 34, 263–276, 1991.
11 B.W. Chappell and J.M. Hergt, The use of known Fe content as a flux monitor in neutron activation analysis, Chem. Geol. 78, 151–158, 1989.
12 W.F. McDonough and M.T. McCulloch, The southeast Australian lithospheric mantle: isotopic and geochemical constraints on its growth and evolution, Earth Planet. Sci. Lett. 86, 327–340, 1987.
13 S.-s. Sun, Chemical composition and origin of the earth's primitive mantle, Geochim. Cosmochim. Acta 46, 179–192, 1982.
14 W.F. McDonough, Constraints on the composition of the continental lithospheric mantle, Earth Planet. Sci. Lett. 101, 1–18, 1990.
15 K.P. Jochum, H.M. Seufert, B. Spettel and H. Palme, The solar-system abundances of Na, Ta, and Y, and the relative abundances of refractory lithophile elements in differentiated planetary bodies, Geochim. Cosmochim. Acta 50, 1173–1183, 1986.
16 K.P. Jochum, W.F. McDonough, H. Palme and B. Spettel, Compositional constraints on the continental lithospheric mantle from trace elements in spinel peridotite xenoliths, Nature 340, 548–550, 1989.
17 S.-s. Sun and W.F. McDonough, Chemical and isotopic systematics of oceanic basalts: Implications for mantle composition and processes, in: Magmatism in the ocean basins, A.D. Saunders and M.J. Norry, eds., pp. 313–345, Geol. Soc. London Spec. Publ., 1989.
18 C. Dupuy, J.M. Liotard and J. Dostal, Zr/Hf fractionation in intraplate basaltic rocks: Carbonate metasomatism in the mantle source, Geochim. Cosmochim. Acta 56, 2417–2424, 1992.
19 R.S. Cohen, R.K. O'Nions and J.B. Dawson, Isotope geochemistry of xenoliths from East Africa: implications for development of mantle reservoirs and their interaction, Earth Planet. Sci. Lett. 68, 209–220, 1984.
20 A.J. Irving, Petrology and geochemistry of composite ultramafic xenoliths in alkalic basalts and implications for magmatic processes within the mantle, Am. J. Sci. 280A, 389–426, 1980.
21 H.G. Wilshire, J.E. Nielson Pike, C.E. Meyer and E.C. Schwarzman, Amphibole-rich veins in lherzolitic xenoliths, Dish Hill and Deadman Lake, California, Am. J. Sci. 280-A, 576–593, 1980.
22 J. Brenan, Partitioning of fluorine and chlorine between apatite and non-silicate fluids at high pressure and temperature, Geophys. Laboratory Yearbook, pp. 61–67, 1991.
23 J.B. Dawson and R. Fuge, Halogen content of some African primary carbonatites, Lithos 13, 139–143, 1980.
24 J. Gittins, The origin and evolution of carbonatite magmas, in: Carbonatites. Genesis and Evolution, K. Bell, eds., pp. 580–600, Unwin Hyman, London, 1989.
25 G. Brey, W.R. Brice, D.J. Ellis, D.H. Green, K.L. Harris and I.D. Ryabchikov, Pyroxene–carbonate reactions in the upper mantle, Earth Planet. Sci. Lett. 62, 63–74, 1983.
26 J.M. Brenan and E.B. Watson, Partitioning of trace elements between carbonate melt and clinopyroxene and olivine at mantle $P-T$ conditions, Geochim. Cosmochim. Acta 55, 2203–2214, 1991.
27 T.H. Green, J. Adam and S.H. Sie, Trace element partitioning between silicate minerals and carbonatite at 25 kbar and application to mantle metasomatism, Mineral. Petrol. 46, in press, 1992.
28 D.R. Nelson, A.R. Chivas, B.W. Chappell and M.T. McCulloch, Geochemical and isotopic systematics in carbonatites and implications for the evolution of ocean-island sources, Geochim. Cosmochim. Acta 52, 1–17, 1988.
29 A. Zindler and E. Jagoutz, Mantle cryptology, Geochim. Cosmochim. Acta 52, 319–333, 1988.
30 P.B. Kelemen, H.J.B. Dick and J.E. Quick, Formation of harzburgite by pervasive melt/rock reaction in the upper mantle, Nature 358, 635–641, 1992.
31 J. Adam, T.H. Green and S.H. Sie, An experimental study of trace element partitioning between peridotite minerals and melts of carbonatite and basanite composition, 1993 (unpubl.).
32 R.J. Sweeney, D.H. Green and S.H. Sie, Trace and minor element partitioning between garnet and amphibole and carbonatitic melt, Earth Planet. Sci. Lett. 113, 1–14, 1992.
33 W.I. Ridley and J.B. Dawson, Lithophile trace element data bearing on the origin of peridotite xenoliths, ankaramite and carbonatite from Lashaine volcano, N. Tanzania, in: Physics and Chemistry of the Earth, L.H. Ahrens, J.B. Dawson, A.R. Duncan and A.J. Erlank, eds., pp. 559–569, Pergamon Press, New York, 1975.
34 Y. Thibault, A.D. Edgar and F.E. Lloyd, Experimental investigation of melts from a carbonated phlogopite lherzolite: implications for metasomatism in the continental lithospheric mantle, Am. Mineral. 77, 784–794, 1992.
35 G.M. Yaxley, D.H. Green and A.J. Crawford, Trace element and Sr-Nd isotopic systematics of carbonatite metasomatised peridotite xenoliths from southeastern Australia, Contrib. Mineral. Petrol., submitted, 1992.
36 F.A. Frey and D.H. Green, The mineralogy, geochemistry

and origin of lherzolite inclusions in Victorian basanites, Geochim. Cosmochim. Acta 38, 1023–1059, 1974.

37 P.B. Kelemen, K.T.M. Johnson, R.J. Kinzler and A.J. Irving, High-field-strength element depletions in arc basalts due to mantle–magma interaction, Nature 345, 521–524, 1990.

38 H.G. Stosch, Zur Geochemie der ultrabasischen Auswürflinge des Dreiser Weihers in der Westeifel: Hinweise auf die Evolution des kontinentalen oberen Erdmantels, PhD Dissertation, Univ. Cologne, 1980.

39 A.R. Wooley and D.R.C. Kempe, Carbonatites: nomenclature, average chemical compositions, and element distribution, in: Carbonatites, Genesis and Evolution, K. Bell, eds., pp. 1–14, Unwin Hyman, London, 1989.

40 J. Gill, Orogenic Andesites and Plate Tectonics, 390 pp., Minerals and Rocks, P.J. Wyllie, ed., Springer-Verlag, Berlin, 1981.

41 W.V. Boynton, Cosmochemistry of the rare earth elements: meteorite studies, in: Rare Earth Element Geochemistry, P. Henderson, ed., pp. 63–114, Elsevier, Amsterdam, 1984.

42 K. Bell and J. Blenkinsop, Nd and Sr isotopic compositions of East African carbonatites: implications for mantle heterogeneity, Geology 15, 99–102, 1987.

43 G.R. Davies and R. Macdonald, Crustal influences in the petrogenesis of the Naivasha basalt–comendite complex: combined trace element and Sr-Nd-Pb isotope constraints, J. Petrol. 28, 1009–1031, 1987.

44 M.J. Norry, P.H. Truckle, S.J. Lippard, C.J. Hawkesworth, S.D. Weaver and G.F. Marriner, Isotopic and trace element evidence from lavas, bearing on mantle heterogeneity beneath Kenya, Philos. Trans. R. Soc. London A297, 259–271, 1980.

45 R. Vollmer and M.J. Norry, Unusual isotopic variations in Nyiragongo nephelinites, Nature 301, 141–143, 1983.

46 R. Vollmer and M.J. Norry, Possible origin of K-rich volcanic rocks from Virunga, East Africa, by metasomatism of continental crustal material: Pb, Nd and Sr isotopic evidence, Earth Planet. Sci. Lett. 64, 374–386, 1983.

47 C. Class, R. Altherr, F. Volker, G. Eberz and M.T. McCulloch, Petrogenesis of Pliocene to Quaternary Basalts from the Huri Hills, northern Kenya, Chem. Geol., in press, 1993.